THE JOURNAL OF PHYSICAL CHEMISTRY B
A JOURNAL OF THE AMERICAN CHEMICAL SOCIETY

pubs.acs.org/JPCB

Article

Frequency Changes in Terminal Alkynes Provide Strong, Sensitive, and Solvatochromic Raman Probes of Biochemical Environments

Published as part of The Journal of Physical Chemistry virtual special issue "Steven G. Boxer Festschrift".

Matthew G. Romei, Eliana V. von Krusenstiern, Stephen T. Ridings, Renee N. King, Julia C. Fortier, Caroline A. McKeon, Krysta M. Nichols, Louise K. Charkoudian, and Casey H. Londergan*

Cite This: *J. Phys. Chem. B* 2023, 127, 85−94

Read Online

ACCESS | Metrics & More | Article Recommendations | Supporting Information

ABSTRACT: The C≡C stretching frequencies of terminal alkynes appear in the "clear" window of vibrational spectra, so they are attractive and increasingly popular as site-specific probes in complicated biological systems like proteins, cells, and tissues. In this work, we collected infrared (IR) absorption and Raman scattering spectra of model compounds, artificial amino acids, and model proteins that contain terminal alkyne groups, and we used our results to draw conclusions about the signal strength and sensitivity to the local environment of both aliphatic and aromatic terminal alkyne C≡C stretching bands. While the IR bands of alkynyl model compounds displayed surprisingly broad solvatochromism, their absorptions were weak enough that alkynes can be ruled out as effective IR probes. The same solvatochromism was observed in model compounds' Raman spectra, and comparisons to published empirical solvent scales (including a linear regression against four meta-aggregated solvent parameters) suggested that the alkyne C≡C stretching frequency mainly reports on local electronic interactions (i.e., short-range electron donor−acceptor interactions) with solvent molecules and neighboring functional groups. The strong solvatochromism observed here for alkyne stretching bands introduces an important consideration for Raman imaging studies based on these signals. Raman signals for alkynes (especially those that are π-conjugated) can be exceptionally strong and should permit alkynyl Raman signals to function as probes at very low concentrations, as compared to other widely used vibrational probe groups like azides and nitriles. We incorporated homopropargyl glycine into a transmembrane helical peptide via peptide synthesis, and we installed *p*-ethynylphenylalanine into the interior of the *Escherichia coli* fatty acid acyl carrier protein using a genetic code expansion technique. The Raman spectra from each of these test systems indicate that alkynyl C≡C bands can act as effective and unique probes of their local biomolecular environments. We provide guidance for the best possible future uses of alkynes as solvatochromic Raman probes, and while empirical explanations of the alkyne solvatochromism are offered, open questions about its physical basis are enunciated.

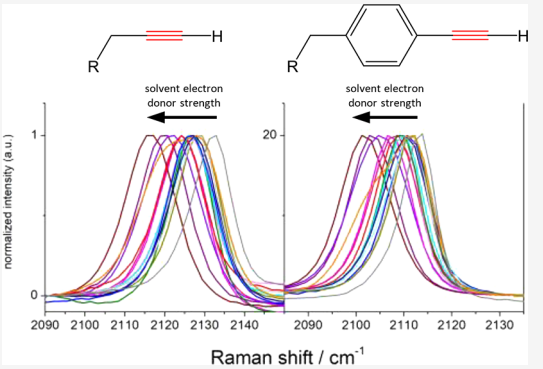

INTRODUCTION

Vibrational spectroscopy can resolve unique structural and dynamic features of biomolecules with very fast intrinsic time resolution compared to more conventional structural techniques. Recent years have seen a great expansion in strategies designed to spectrally isolate specific sites of proteins and other biomolecules in their vibrational spectra. Site-directed isotopic substitution is one approach that has been used to spectrally label specific sites on protein backbones[1−10] and side chains[11−19] as well as entire segments of proteins.[20,21] Another recently widespread approach is the placement and/or interrogation of unique functional groups that either appear in the "clear" region of vibrational spectra between 1900 and 2700 cm^{-1} or have unique vibrational frequencies that can be viewed through difference spectroscopy of labeled vs unlabeled samples.[22,23] Artificial vibrational probe groups of interest have included nitriles,[24] cyanates[25] and thiocyanates,[26] azides,[27] and nitro groups,[28] which all generally have the advantage of being much smaller than probe functionality for other techniques like fluorescence and electron paramagnetic resonance, as well as larger metal carbonyl vibrational labels.[29,30] A major challenge for each of these vibrational labeling strategies is the detection of isolated vibrations from samples with very low, biologically relevant concentrations of a biomolecule of interest: ideally such probes would be viewable *in vitro* at tens of μM or lower

Received: August 29, 2022
Revised: November 19, 2022
Published: December 20, 2022

concentration, which is well below the detection thresholds of most of these current probes despite the currently broad variety of infrared (IR) and Raman-based instrumentation.

These unique, site-specific molecular vibrations in biomolecules have been interrogated using IR absorption spectroscopy, resonant IR nonlinear optical techniques,[31] and continuous-wave[19,32] and higher-order, time-resolved[33] variants of Raman spectroscopy.[34] The majority of recent work in this area has focused on IR spectroscopy, although there have been many indications from the imaging community that Raman spectroscopy might actually lead to a lower detection threshold for certain vibrations due to greater flexibility in both optical sampling and instrumental design and the possibility of ultraviolet- (UV-) resonant enhancement for signals associated with aromatic side chains[33,35,36] or stimulated Raman scattering for spectrally isolated signals.[33,37]

One functional group of increasing interest is the terminal alkyne, whose C≡C stretching band appears between 2000 and 2250 cm^{-1} depending on its covalent structural neighbors. This functional group is only weakly dipolar (if at all), and there is not a large transition dipole associated with absorptive excitation of the C≡C stretching vibration. However, there is a large polarizability change associated with excitation of the same stretching mode, thus terminal alkynes have been shown to have strong Raman signals. Classic work by Alaune et al.[38−40] and more recent work by Sodeoka and co-workers[36] indicated that the C≡C stretching Raman shifts of terminal alkynes can be quite strong compared to other normal modes in the same frequency window (or throughout the biomolecular Raman spectrum), with large scattering intensities that increase substantially upon conjugation of the alkyne to any neighboring π system.

Alkynes have been implemented as minimally sized spatial imaging labels in Raman microscopy by the Sodeoka group[36,41−45] and in stimulated Raman microscopy in the Min and Wei groups,[33,37,46−49] and deuteration and other synthetic variation around the alkyne groups has been used to create groups of multiplex probes with sufficiently spaced-out C≡C stretching frequencies.[46,50,51] These imaging studies have largely presupposed the frequency insensitivity of the alkyne groups' Raman frequencies to their local environments. While very recent work has used the frequency shift of the terminal alkyne group upon deuteration (a chemical change) to provide evidence of site-specific solution exposure,[49,50] frequency *variations* of an intact alkyne group have not been broadly used as an additional site-specific observable. Amidst all of this reported imaging work, two recent *in vitro* studies used alkyne functional groups on alpha-synuclein[32] and acyl carrier proteins[52] to draw conclusions related to proteins' site-specific functional structures and dynamics, and silyl-derivatized alkynes have been proposed as possible solvatochromic IR probes.[53,54] The main goal of the current work is a comprehensive solvatochromic overview of the response of the frequencies and lineshapes of the C≡C stretching bands from terminal alkynes to the alkynes' local structural environments, for use as both imaging probes and as *in vitro* protein-based probes of proteins' dynamics and interactions.

Terminal alkynes have been introduced into many biomolecules in recent years as a precursor to the bioorthogonal Huisgen 3 + 2 cycloaddition reaction with azides, a widely used "click chemistry" reaction.[55] Due to the popularity of the "click" approach, many alkyne-containing biomolecular precursors are commercially available and can be incorporated into biopolymers via a number of strategies. In proteins, γ-ethynylhomoalanine (also called homopropargyl glycine, "HPG", which contains an aliphatic terminal alkyne) can be incorporated recombinantly as a methionine proxy using an auxotrophic *Escherichia coli* strain.[56] *p*-ethynylphenylalanine (pCC-Phe) can also be recombinantly incorporated into protein sequences using "amber" stop codon suppression coupled with a tRNA synthetase that was evolved to recognize and incorporate 4-substituted phenylalanine derivatives.[57,58] A number of other commercially available, terminal alkyne-containing amino acids can be incorporated into peptides via fmoc-based solid-phase peptide synthesis, and new techniques for alkyne inclusion into biomolecules continue to proliferate.[44]

Although there are already many alkyne-labeled proteins and biomolecules reported in the literature, there has been relatively little systematic work to document the dependence of the alkyne C≡C stretching frequency on the probe group's local environment.[32,52−54] Terminal alkynes do not participate in hydrogen bonding, so it is likely that any variation in C≡C frequencies in biomolecules will come solely from some combination of electrostatic factors (i.e., the local electric field or multipolar environment) and more direct electronic interactions (like dispersion and exchange-repulsion interactions).[59−61] The alkynyl could be a hydrophobic complement to nitriles and azides, whose polarity could make them difficult to place in hydrophobic environments without perturbation and whose unique vibrations are strongly complicated[62−64] and somewhat more clearly defined,[65] respectively, by local hydrogen bonding interactions. Here we fully document the frequency dependence of the alkynyl C≡C stretching band of both aliphatic and aromatic alkynes on the environment around the probe atoms. We also establish our own rough detection limits for this vibration in both IR and Raman spectroscopy, toward analytical work at low concentrations of alkynyl-labeled biomolecules.

This work uses the model compounds propargyl acetate (**1**) and *p*-ethynylbenzyl alcohol (**2**) to document the relative IR and Raman intensities and environment-dependent frequency variations for aliphatic and aromatic terminal alkynes, respectively. These models were chosen due to their high solubilities in most solvents of interest and the lack of any observed solute clustering in all solvents. (We also collected many IR and Raman spectra of propargyl alcohol (**3**), but ultrafast IR experiments not included here suggested that this compound clustered at very high concentrations, so we moved to propargyl acetate as the main model compound for aliphatic alkynes. Some data for **3** appear in the Supporting Information.) We use the free amino acids **4** and **5** to establish rough Raman sensitivity limits in aqueous buffer for comparison to similar practical *in vitro* intensity limits of other common probe groups. (Structures for all model compounds and amino acids are shown in Figure 1.) We then applied Raman spectroscopy to a model peptide with an HPG residue and a model protein with a pCC-Phe residue to demonstrate solvatochromic Raman spectroscopy of the alkynyl C≡C stretching vibration as a site-specific probe in proteins.

EXPERIMENTAL METHODS

Materials. **1** and **2** were obtained from Sigma-Aldrich and used as received. **3** was obtained in a SureSeal bottle from Aldrich and transferred via syringe. **4** was obtained from

https://doi.org/10.1021/acs.jpcb.2c06176
J. Phys. Chem. B 2023, 127, 85−94

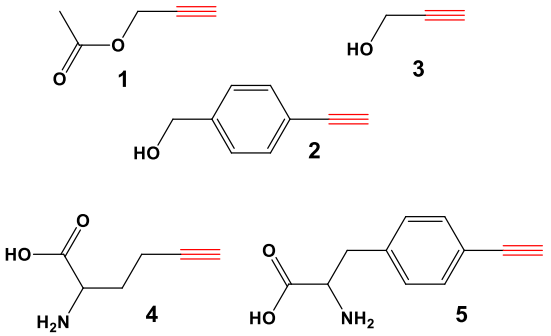

Figure 1. Structures of propargyl acetate (**1**), 4-ethynylbenzyl alcohol (**2**), propargyl alcohol (**3**), *β*-ethynyl alanine (**4**), a.k.a. homopropargyl glycine (HPG), and *p*-ethynyl phenylalanine (**5**) (pCC-Phe).

Chiralix, Inc. and used as received. **5** was synthesized following a published procedure.[58] All organic solvents were obtained from either Sigma/Aldrich or PharmCo-Aaper and used as received, except for THF, which was used directly from a pressurized and dry keg from Acros, and triethylamine, which was freshly distilled before use.

Production of the peptide and protein samples is described in the Supporting Information.

Infrared Spectroscopy. All IR spectra were collected using a Vertex 70 FTIR spectrometer (Bruker Optics), with a photovoltaic MCT detector (Kolmar Technologies). All IR spectra presented here were acquired in 64 or 128 scans at 2 cm^{-1} resolution. All liquid samples were placed in a 22 μm fixed-path length CaF_2 BioCell (BioTools, Inc.). For all liquid samples the neat solvent was used as the background, and in a few cases further baseline correction around the C≡C stretching peak was performed by excluding data from 2090 to 2140 cm^{-1}, fitting the surrounding spectrum to a polynomial, and subtracting the fit from the data. Samples of **1** were at 100 mM concentration and samples of **2** were at 500 mM.

Raman Spectroscopy. All Raman spectra were collected using a home-built CW Raman spectrometer described elsewhere:[19,66] detection hardware consists of a PI-Acton Spec-10/100 liquid N_2-cooled CCD camera attached to a PI-Acton SpectraPro 500 mm single monochromator. The monochromator slit, 600 grooves/mm grating and *f*-matched entrance optics yield a spectral resolution of 3.0 cm^{-1} in the configuration used for all spectra reported here.

Samples of **1**−**5** were made in glass vials at approximately 1 mL scale; all samples of **1**−**5** were exposed at least twice for reproducibility. A few microliters of all samples of **1**−**5** were placed in 1 mm capillary tubes and excited vertically using a 532 nm DPSS laser (Cobolt, Inc.) attenuated to 80 mW incident CW power and focused vertically through the transparent sample. Scattered light was collected at 90 degrees vs the excitation beam direction. Rayleigh scattering was rejected at the monochromator entrance slit using a long-pass filter at 532.0 nm (Edmund Optics). Samples of **1**−**3** at 100 mM concentration were collected in single accumulations of 1−30 s. Experimental details for data collected at lower concentrations for **4** and **5** and for peptide and protein samples are reported below.

RESULTS AND DISCUSSION

IR Spectroscopy of Model Compounds. IR spectra of **1** and **2** in a range of solvents are displayed in Figure 2. Solvents

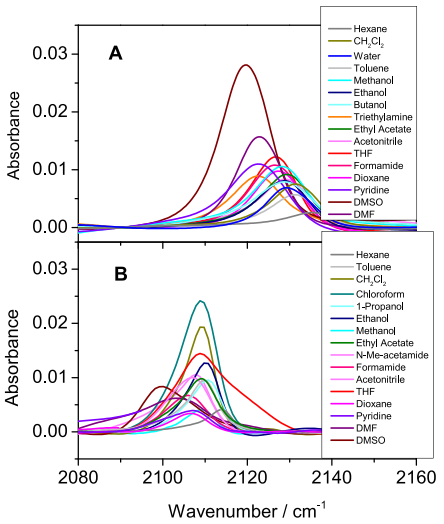

Figure 2. C≡C stretching region IR spectra of 100 mM **1** (A) and 500 mM **2** (B) in various solvents. Solvent absorptions were subtracted through use of pure solvent as the background and further baseline correction. Note the substantially weaker molar absorbance from **2** and the generally weak signals in each case. The legends are ordered from highest to lowest frequency.

were chosen to provide a range from nonpolar to polar and H-bonding (both donors and acceptors) to non-H-bonding. Systematic variations in intensity, line width, and frequency of the C≡C stretching band were observed across this range of solvents for both compounds, but the most relevant feature of these data for prospective alkyne IR probes was the weak oscillator strength and resultingly small IR absorption signal. The spectra in Figure 2 are solvent-subtracted, and the weakness of the C≡C stretching signals compared to the solvent background slightly distorts some of the lineshapes at the level of solvent subtraction applied to the data in Figure 2.

We arrived quickly at the conclusion that alkyne probes will not be useful at the low concentrations necessary for *in vitro* experiments on proteins or other common biomolecules nor at the even lower concentrations expected *in vivo*. The average alkyne extinction coefficient we measured across these solvents for **1** is about 13 M^{-1} cm^{-1} and the same value for **2** is about 3 M^{-1} cm^{-1}, which means that concentrations in the tens to hundreds of mM would be needed to reproducibly capture these signals via IR absorption at a signal:noise level attainable by the best current detectors. Such high concentrations are not feasible for most biomolecular samples. This conclusion was also reached by Kossowska et al., who endeavored to increase the C≡C infrared oscillator strength through further functional group substitution.[54] However, it is very clear in Figure 2 that there is a substantial variation (over a frequency range about as wide as the line width) of the C≡C stretching frequencies of both aliphatic and aromatic terminal alkynes in different solvent environments. While there also appears to be a substantial "non-Condon-like" dependence of the band's oscillator strength on the frequency, with lower-frequency bands (mainly in the most polar solvents) being substantially more intense than those at higher frequencies, even the most intense bands for **1** are not strong enough for use at the low-mM and sub-mM concentrations necessary for collecting IR spectra of proteins.

Raman Spectroscopy of Model Compounds. Figure 3 shows intensity-scaled Raman spectra in the C≡C stretching

https://doi.org/10.1021/acs.jpcb.2c06176
J. Phys. Chem. B 2023, 127, 85−94

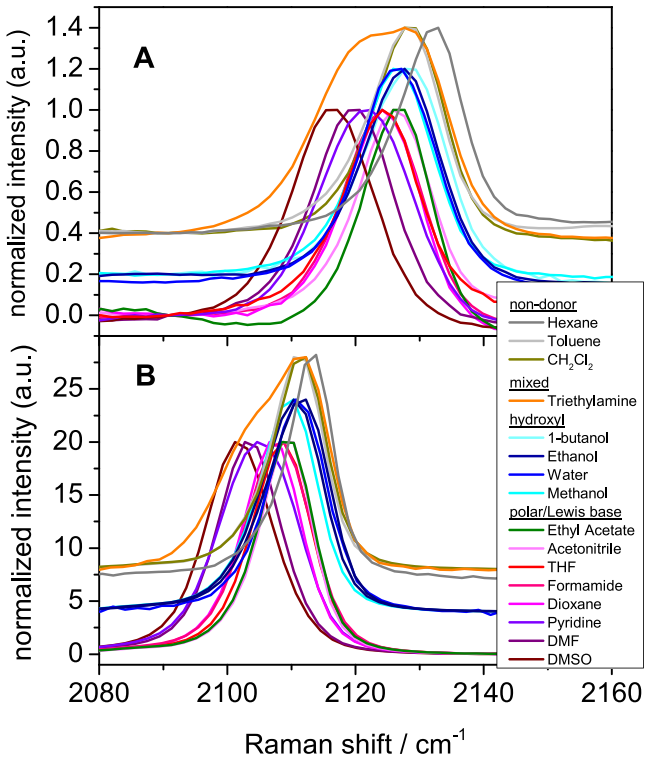

Figure 3. Peak-intensity-normalized Raman spectra in the C≡C stretching region of 100 mM **1** (A) and 100 mM **2** (B) in various solvents, with no spectral corrections applied other than subtraction of dark current/baseline offset. (The concentrations of **2** in water and hexane are substantially lower than 100 mM due to solubility issues, but the signals are still quite clear without additional data manipulation.) The legend is ordered from highest to lowest frequency, and solvents are vertically offset into three groups and colored according to those groups: nonelectron donors, hydroxyl-containing solvents, and polar/Lewis base solvents. Triethylamine is discussed below.

region for **1** and **2** in a similar range of solvents. Aside from scaling the intensities to a shared maximum peak value, the spectra in Figure 3 are unprocessed except for subtraction of the offset counts from the CCD array detector. In each spectrum, the C≡C peak was very strong and quite obvious without any removal or manipulation of any baseline solvent signals in this spectral region. It was immediately clear from our short, uncorrected Raman exposures that these peaks are both very strong, especially the signals from **2**: please see further below for discussion of our measured sensitivity limits for aliphatic and aromatic alkyne stretching bands at low concentrations.

The frequencies of each C≡C stretching band depend on the solvent in systematic ways that appear at first glance to depend mainly on the polarity of the solvent. The range of central frequencies is nearly equal to that of the mean C≡C line width. Hydrogen bonding from protic solvents does not appear to be a strong factor in determining the C≡C stretching frequency. Across the range of solvents, the peak intensities and line widths of the C≡C stretching bands for **2** are somewhat anticorrelated, but the integrated intensity of the C≡C peak remains about the same across each data set when compared to an appropriate internal standard peak from **2**: this invariance of the integrated intensities suggests that there is *not* a Raman "non-Condon" effect for this vibration where the scattering cross-section depends on the frequency, as the oscillator strength does for the IR absorption of the C≡C stretching band.

In Figure 3, as the C≡C frequency decreases, the spectral line width for each model compound increases substantially. All the lineshapes in Figure 3 are quite symmetric and approximately Gaussian in shape, and broader frequency distributions occur in solvents with a lower average frequency. This suggests that the factors that most strongly affect the frequency also define the inhomogeneous distributions of frequencies represented in the C≡C stretching lineshapes. C≡C bands with lower mean and mode frequencies generally have broader line widths (and slightly lower peak intensities for **2**): this is consistent with the C≡C lineshapes' reporting an inhomogeneous distribution of frequencies that broadens with solvents that interact more strongly with the electronic structure of the vibrational chromophore. The C≡C frequencies and line widths (and peak intensities for **2**) all correlate with empirical solvent scales in similar ways. One solvent that leads to broader lineshapes compared to any other solvent in our data set is triethylamine, which we comment on below.

We used an extensive list of reported solvent parameters, some of which are empirical solvent scales and some of which are basic physical liquid or molecular properties of each solvent, to estimate empirically what physical phenomena most strongly affect the C≡C stretching frequency (please see the Supporting Information for a list of considered parameters and a few representative single-parameter correlation plots). The single empirical solvent parameter with the strongest correlation to the frequencies from Figure 3 was the Koppel–Palm Lewis basicity.[67] In a broad sense, stronger correlations with the frequency were observed for parameters associated with electron donor strength and, more generally, the electronically polarized or polarizing nature of the solvent: more polarized or polarizing solvents always lead to lower mean C≡C stretching frequencies across our large solvent set.

However, this "dipoles" dependence does not mean that there is a strong correlation with empirical estimates of the electric field: the Onsager reaction electric field parameter,[68] for example, is essentially uncorrelated with the solvatochromic C≡C stretching frequency for either **1** or **2** (see Figure S3). In considering single empirical parameters one at a time, it appears that local interactions with electron donors, rather than longer-range electrostatic fields and interactions, are the most important single determinant of the alkyne stretching frequency. These local interactions with electron donors most likely influence the C≡C stretching potential surface through quantum mechanical dispersion or exchange-repulsion effects (as appears to be the case as well for nitriles[69]) rather than through Coulombic/electrostatic interactions.

Comparison to a reduced set of four essential meta-reduced solvent parameters[70] (Figure 4) suggests several empirical conclusions about the physical root of solvatochromism in the terminal alkyne C≡C stretching frequency. H-bonding donor and acceptor coefficients in our predicted frequency fits nearly cancel each other out, but the nonzero coefficients for each of these aggregate parameters indicate that the C≡C frequency does depend substantially on local interactions with functional groups that would otherwise participate in H-bonds with reasonable partners. Both the reduced "dispersion" and "electrostatic" parameters contribute to some extent to the C≡C frequency for both aliphatic and aromatic terminal

https://doi.org/10.1021/acs.jpcb.2c06176
J. Phys. Chem. B 2023, 127, 85−94

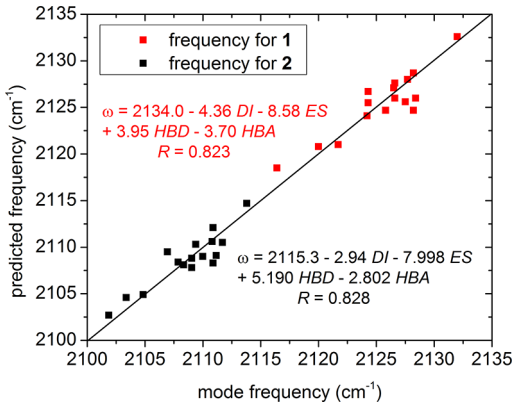

Figure 4. Comparison between alkyne stretching frequencies for **1** (red) and **2** (black) in 16 solvents and the frequencies predicted by best fits to a linear combination of four reduced solvent parameters from the analysis of Laurence et al.[54] The linear combinations are displayed on the plot with the correlation coefficient from each fit: "*DI*" is the dispersion parameter, "*ES*" is the electrostatic parameter, "*HBD*" is the H-bond donor parameter, and "*HBA*" is the H-bond acceptor parameter. The diagonal (which would signify a 1:1 match between actual and best-fit frequencies) is shown as a visual guide.

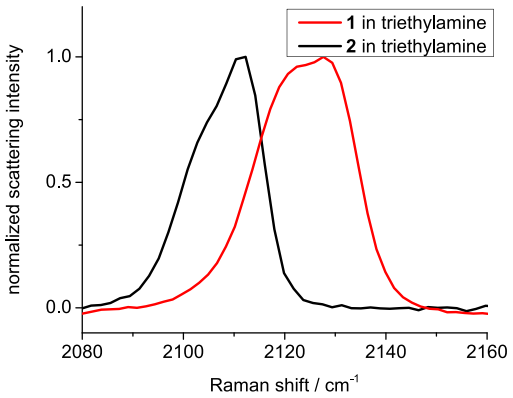

Figure 5. Alkyne stretching Raman spectra of **1** and **2** in triethylamine: data from Figure 3 presented for clarity. Decomposition/fitting to two populations and temperature dependence appear in Figures S5 and S6.

alkynes, which suggests empirically that alkyne frequencies could report both local and longer-range electronic effects.

The ability of H-bond donors and acceptors to influence the C≡C frequency does not suggest that alkynes are participating in weak H-bonds with the solvent; it is rather more likely that the (very localized) exchange repulsion and dispersion interactions are partly included in the H-bonding meta-parameters, as well as in the "dispersion" and "electrostatic" meta-parameters in this aggregated solvent scale. Further comparison to individual empirical solvent scales is certainly possible, but such comparisons would only be of limited use in describing the more anisotropic environments that might be encountered for alkyne probes in biomolecular environments. A more physically based assessment, perhaps based on fragment potential-based frequency calculations formulated by Blasiak and Cho,[59−61] would provide a more directly quantitative assessment of the exact physical factors that govern the alkyne stretching frequency in specific biomolecular circumstances. But the empirical comparison here to published solvent scales does indicate that alkyne frequencies depend strongly on several physical (mainly electronic) factors in the alkyne's local environment.

We paid special attention to alkyne bands for **1** and **2** in triethylamine, in which each model compound exhibits a relatively high C≡C mode frequency, but also to a very broad line width that stretches down to frequencies otherwise observed in much more polar solvents. These alkyne stretching bands in triethylamine appear in Figure 5, and we decomposed these bands into two possible spectral subpopulations and performed temperature dependent experiments whose results appear in the Supporting Information (Figures S5 and S6). The odd lineshapes and our analysis may shed some light on the local nature of the interactions that influence the C≡C frequency in that solvent. Triethylamine is an electronically and chemically anisotropic molecule: one end of it is a strong H-bond acceptor and electron donor (the nitrogen atom), while the other end (the ethyl groups) presents an alkane-like environment. It appears that probe-bearing molecules are sensitive to this dual nature of the solvent: alkyne groups in contact with the electron donor N atom should have lower frequencies, while alkyne groups surrounded by ethyl groups can display frequencies closer to those observed in hexane. The broad, asymmetric inhomogeneous line shape for both **1** and **2** in triethylamine apparently comes from this dramatic difference between the electronic interactions of the alkyne probe with either end of the solvent molecules. Fitting of both the bands in Figure 5 to two Gaussians (Figure S5) suggests that these bands could each be decomposed into a broad, low-frequency component consistent with electron donors interacting with the alkyne and a narrow, higher frequency component consistent with the alkyne residing in a non-interacting alkane-like environment. Temperature-dependent spectra (Figure S6) displayed only small changes, suggesting that if there are two subpopulations, they are not strongly enthalpically distinct. Determining a truly physical and nonempirical explanation for these exceptional lineshapes in triethylamine is likely to require detailed simulation studies at multiple levels of theory, and it is a subject for future computational work.

Without further quantitative analysis or empirical comparisons, there are two important practical conclusions for possible use of alkynes in biomolecules that are evident in the solvent-dependent frequencies of the C≡C stretching bands from Figure 3. The first conclusion is that the central C≡C frequency of a single species could vary by as much as 15−20 cm^{-1} in biologically relevant environments: while the homogeneous solvents used here encapsulate many relevant functional groups, specific local electronic interactions could lead to potentially broader shifts than we have observed in these relatively simple environments. This possibility of large frequency variations is very important information to consider when the C≡C stretching band is used as a probe in Raman microscopy: hyperspectral images that fixate on signals of only one frequency might miss some shifted alkynyl signals and misrepresent the spatial distributions of alkyne-labeled molecules if those molecules undergo changes in their immediate environments. This could also be an experimental issue for stimulated Raman imaging,[33,37] which most typically relies on a narrow-band Stokes pulse with very specific frequency matching that could miss or under-stimulate (and thus under-count) some of the C≡C frequencies in a sample if there is substantial variation in the environments and vibrational frequencies of the C≡C groups.

https://doi.org/10.1021/acs.jpcb.2c06176
J. Phys. Chem. B 2023, 127, 85−94

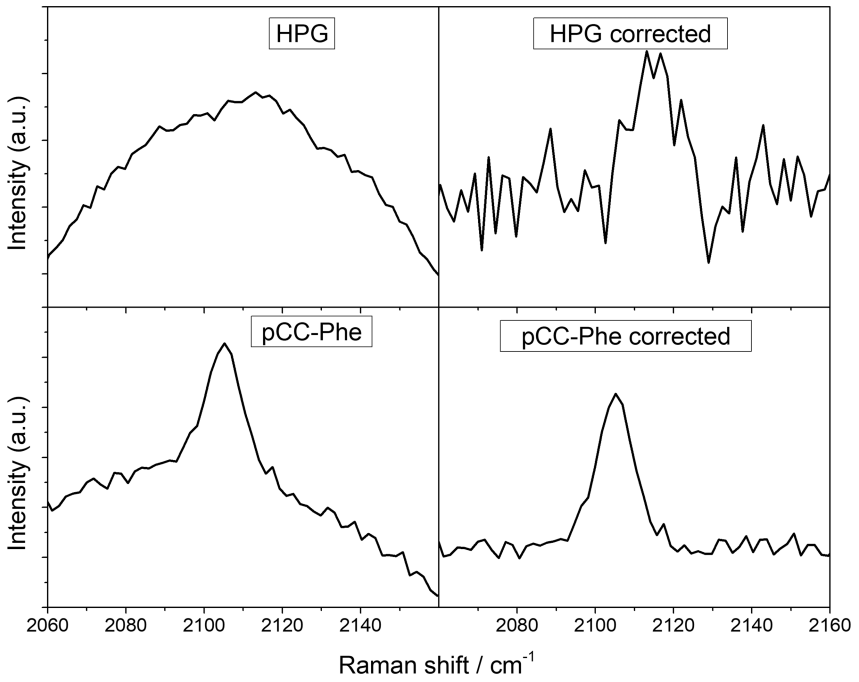

Figure 6. Representative low-concentration Raman spectra for alkyne-containing amino acids in aqueous buffer. (Top row) C≡C stretching region Raman spectrum for 50 μM compound **4**, collected using our home-built, nonresonant CW Raman spectrometer with a total exposure time of 2 h. Raw and baseline-corrected spectra are shown. (Bottom row) C≡C stretching region Raman spectrum for 5 μM compound **5**, collected using the same instrument with the same total exposure time. We expect that stimulated Raman instruments or other more optically optimized instruments will be capable of collecting similar signals in a fraction of our exposure time: these spectra are presented as an indication that solvatochromic alkyne signals can be clearly distinguished at much lower concentrations than for most other vibrational probe groups (and all current IR probes).

The second conclusion from the data in Figures 3 and 4 is that the C≡C frequency reports directly and with high sensitivity on the alkyne group's local electronic environment. This means that alkynes could provide a practical complement to nitriles and azides, whose frequencies are more strongly determined by the local presence of water and other H-bond donors.[22,27,65,69,71] Alkyne C≡C stretching bands are likely to be clearer electronic reporters than C≡N or N═N═N stretching bands in strongly polarized environments like the active sites and interiors of well-structured proteins; the only complication for direct comparison with nitrile or azide probes is that C≡C bands are best collected via Raman scattering rather than IR absorption techniques. (Both nitrile and azido probe bands are also easily collected via Raman scattering, so perhaps the best one-dimensional spectral experiment for all these probe groups together will be Raman scattering rather than IR absorption.)

Sensitivity Limit. CW-excited spontaneous Raman spectra were collected for successive dilutions of **4** and **5** in buffered aqueous solution. A representative low-concentration spectrum for each amino acid is shown in Figure 6. With hours-long collections at incident powers below 100 mW and relatively low power densities compared to those typically achieved in Raman microscopy, the C≡C stretching bands of **4** and **5** are clearly visible at concentrations of 50 μM and 5 μM, respectively. This clear visibility at such exceptionally low concentrations under low-peak power CW excitation conditions, especially for **5**, stands in great contrast to the typical limits at which nitriles and azides can be clearly seen in the IR or even in resonant or stimulated Raman experiments (typically hundreds of μM or more typically low-mM concentrations). Our home-built sampling apparatus still includes a lot of flexibility to further decrease the concentration at which these signals could be collected beyond the spectra in Figure 6, and we have not implemented any enhancement techniques (i.e., plasmonic substrates, extra beams or ultrafast-pulse stimulation, UV resonance, etc.). The strong C≡C signals enable alkyne probe groups to be applied to much lower *in vitro* concentrations of proteins than for other vibrational probe groups. The unique strength of the C≡C stretching band from **5** suggests that pCC-Phe or other aromatic alkynes (in small compounds like "EdU"[42] and its successors[44]) could be applied at concentrations more commonly used for fluorescence experiments than for other vibrational probe groups, and the relatively small structural perturbation (only two additional atoms as compared to native Phe residues, or one compared to native Tyr residues) suggests that aromatic alkynes could be useful in new locations on proteins (possibly associated with intermolecular interactions) as compared to other larger, nonvibrational probe groups used for fluorescence, paramagnetic resonance, or other techniques.

Across the range of prepared concentrations, the observed C≡C frequencies of **4** and **5** were not concentration-dependent and were consistent with the frequencies of **1** and **2** in water. We expect that the solvent-dependent frequencies from Figure 3 should be reasonably applicable (at least to a first approximation) to interpretation of spectra for **4** and **5** when they are incorporated into proteins or other biomolecules, with a small systematic inductive shift taken into account for the aliphatic alkynes of **1** vs HPG residues in peptides and proteins.

Site-Specific Raman Spectroscopy in Peptides and Proteins. Alkyne-containing amino acids were successfully incorporated into two biomolecular systems, and Raman spectra were collected for the alkyne C≡C stretches (Figure 7). HPG was incorporated into a hydrophobic transmembrane

https://doi.org/10.1021/acs.jpcb.2c06176
J. Phys. Chem. B 2023, 127, 85−94

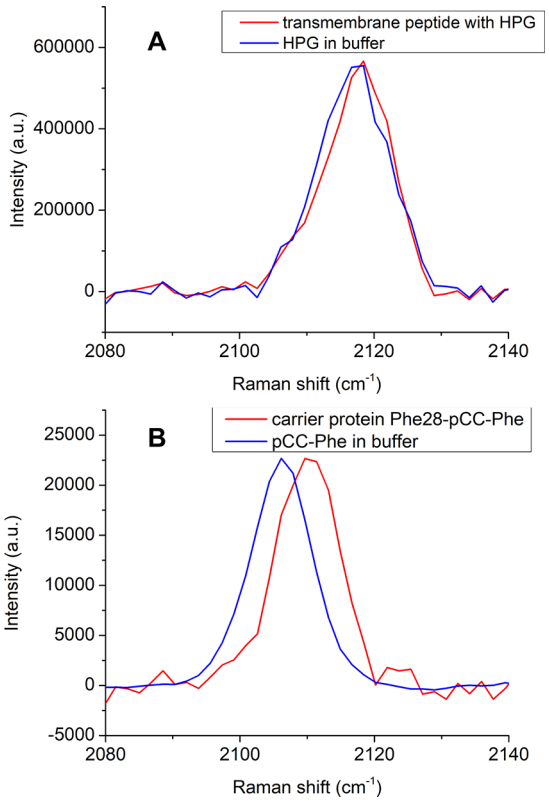

Figure 7. Representative Raman spectra for alkyne-containing amino acids in peptides and proteins. (A) Baseline-subtracted C≡C stretching region Raman spectrum for 2.5 mM HPG-containing transmembrane peptide inserted into 50 mM POPC large unilamellar vesicles. This spectrum used 80 mW, 532 nM excitation and was collected for 2.5 h. (B) Baseline-subtracted C≡C stretching region Raman spectrum for the *E. coli* fatty acid carrier protein with with pCC-Phe incorporated at Phe28 via stop codon suppression (red), compared to pCC-Phe dissolved in buffer solution. These spectra used the same excitation conditions and were collected for 30 s.

peptide via solid-phase peptide synthesis, and that peptide was inserted into the bilayer of 1-palmitoyl-2-oleoyl-sn-glycero-3-phosphocholine (POPC) vesicles (Figure 7A). pCC-Phe was incorporated in place of Phe28, a key amino acid in the *E. coli* fatty acid acyl carrier protein ("AcpP"), using the "amber" stop codon suppression/genetic code expansion technique,[57,58] and we collected a Raman spectrum in the C≡C stretching region for this purified protein (Figure 7B).

We placed HPG in the transmembrane helical peptide to begin to evaluate the usefulness of this probe group in a membrane environment. A complementary circular dichroism spectrum (see Figure S7) indicates that the peptide is folded into a helix as anticipated, and thus we also presume that the peptide was successfully inserted into the membrane during a mutual rehydration process with the POPC lipids (see Supporting Information, Methods). HPG in this sequence is located directly in the center of a model peptide whose hydrophobic length was designed to match the hydrophobic thickness of POPC bilayers, so the probe amino acid should be directly in the center of the lipid bilayer (an environment dominated mainly by alkane chains). However, the mode frequency (2118 cm^{-1}) of the observed C≡C stretching vibration nearly matches that of **4** in buffer, which appears at 2117 cm^{-1} with a similar full width at half-maximum (about 11.5 cm^{-1} for the HPG peptide probe and 12.0 cm^{-1} for **4** in buffer solution).

The near-aqueous frequency observed for HPG in the transmembrane peptide suggests a somewhat electronically polarizing environment inside the bilayer for HPG, so it may be that the alkyne here is reporting on local bilayer electrostatics in the absence of any strongly electron-donating groups in its local vicinity. Ongoing work with HPG at varying burial depths in similar peptides will be used to explain this provocative observation in Figure 7A, but for now this data demonstrates that the Raman spectrum of incorporated HPG can report on its microenvironment in a model peptide at relatively low concentration.

This observation of very little shift to higher frequency than the solvent-exposed alkyne frequency is in contrast to previously reported Raman signals for aliphatic alkyne probes attached to the phosphopantetheine (Ppant) arms of several carrier proteins, which shifted to higher frequency by about +5 cm^{-1} when sequestered inside a very hydrophobic cavity of the protein.[52] This indicates that the interior of a lipid bilayer and a hydrophobic pocket inside a protein are substantially different molecular environments from the point of view of the terminal alkyne probe group.

The clear C≡C stretching band for pCC-Phe in the acyl carrier protein (Figure 7B) reports a significantly different frequency than that of **5** in buffer. The native Phe28 residue in this protein (see Figure S8 for the structure) is located at the mouth of the hydrophobic channel that this carrier protein can use to sequester its growing substrate, which is covalently attached to the end of its Ppant arm (which has been observed to swing into a position that contacts Phe28 as well as several other residues[72]). The relatively high frequency observed for pCC-Phe in Figure 7B appears to report a largely nonpolar and solvent-excluded environment free of strong electron donors, and this site could be used in the future to show changes in the carrier protein's structure as the protein and its Ppant arm sample different conformations.

The protein spectrum in Figure 7B is for a sample that is approximately 100 μM concentration, and it is likely according to Figure 5 that much lower concentration samples could yield similar results. pCC-Phe residues are relatively easily incorporated recombinantly into proteins using the same tRNA synthetase plasmid that can incorporate other para-substituted phenylalanine derivatives,[58,73,74] and Figure 7B provides a first glimpse of how this residue can serve as a very intense and strongly solvatochromic vibrational probe group (rather than just as a fluorophore[58]).

The two observations in Figure 7 of alkyne-labeled Raman probe amino acids in biomolecular systems demonstrate that terminal alkynes are very promising solvatochromic probes of their local environments in proteins. We look forward to further site-specific application of alkynes as solvatochromic vibrational probe groups: the model compounds data in Figures 2−5 suggest that these probes may be best situated in highly polarized environments like active sites, the interiors of folded proteins, and at interfaces whose functions are strongly defined by electronic influences (such as protein−membrane interfaces or electrostatically or otherwise electronically driven protein−protein interfaces). The recent observation of shifts associated with hydrophobic sequestration of the alkyne probe[52] also demonstrates that in some cases, the alkyne group's frequency could also report on changes in solvent exposure. Due to the strong solvatochromism of all terminal

https://doi.org/10.1021/acs.jpcb.2c06176
J. Phys. Chem. B 2023, 127, 85−94

alkynes and their sensitivity to local electronic interactions, it is likely that C≡C stretching band frequencies would change if the probes were placed on the "outside" of biomolecules that transit through cellular compartments with different compositions or solvent environments, so alkynes might also be useful solvatochromic probes for observing the spatially dependent environments around molecules of interest in future imaging experiments.

CONCLUSIONS

The C≡C stretching bands of terminal alkynes are very weak IR absorbers, but they provide strong and clear signals in Raman scattering spectra. Aromatic alkynes are especially strong Raman scatterers, and we could detect a signal from an aromatic amino acid model compound at below 10 μM concentration, an unprecedented sensitivity limit compared to other vibrational probe groups. These strong and clear signals will enable the placement of alkynes as probe groups in many proteins that might be inaccessible to other vibrational labels. They also support the notion that alkynes are excellent label groups for Raman imaging, a suggestion already realized by others, but without consideration of their notably broad solvatochromism.

Solvent-dependent Raman spectra show that the C≡C frequencies of terminal alkynes are strongly sensitive to their local environments. Electron donating parameters for many solvents exhibit the best correlations with average C≡C frequencies, and lower-frequency C≡C frequencies with broader line widths are observed in more strongly electron-donating and polarizing solvents. The mostly inhomogeneous line width appears to reflect the local distribution of solvent molecules around the probe group. The frequency dependence of the C≡C stretching band should be considered if alkynes are to be implemented as labels for imaging studies.

Several alkyne-containing amino acids can be incorporated into proteins, and the strong solvatochromism of the C≡C stretching band suggests that it can be used as a probe of the changing environments around specific sites in proteins. The best application of such probes might be to the interiors or active sites of proteins, since the C≡C band's frequency does not report strongly on the presence of solvent (except for distinguishing between solvent-exposed and very hydrophobic, nonpolarized environments) but otherwise can vary widely due to changes in local electronic factors.

ASSOCIATED CONTENT

Supporting Information

The Supporting Information is available free of charge at https://pubs.acs.org/doi/10.1021/acs.jpcb.2c06176.

Representative spectra for propargyl alcohol, a list of solvent parameters compared to our data with representative single-parameter correlation plots, temperature-dependent spectra in triethylamine, and methods associated with peptide and protein samples (PDF)

AUTHOR INFORMATION

Corresponding Author

Casey H. Londergan − *Department of Chemistry, Haverford College, Haverford, Pennsylvania 19041-1392, United States;* orcid.org/0000-0002-5257-559X; Email: clonderg@haverford.edu

Authors

Matthew G. Romei − *Department of Chemistry, Haverford College, Haverford, Pennsylvania 19041-1392, United States*

Eliana V. von Krusenstiern − *Department of Chemistry, Haverford College, Haverford, Pennsylvania 19041-1392, United States;* orcid.org/0000-0002-9569-3262

Stephen T. Ridings − *Department of Chemistry, Haverford College, Haverford, Pennsylvania 19041-1392, United States*

Renee N. King − *Department of Chemistry, Haverford College, Haverford, Pennsylvania 19041-1392, United States*

Julia C. Fortier − *Department of Chemistry, Haverford College, Haverford, Pennsylvania 19041-1392, United States*

Caroline A. McKeon − *Department of Chemistry, Haverford College, Haverford, Pennsylvania 19041-1392, United States*

Krysta M. Nichols − *Department of Chemistry, Haverford College, Haverford, Pennsylvania 19041-1392, United States*

Louise K. Charkoudian − *Department of Chemistry, Haverford College, Haverford, Pennsylvania 19041-1392, United States;* orcid.org/0000-0002-4342-2815

Complete contact information is available at: https://pubs.acs.org/10.1021/acs.jpcb.2c06176

Author Contributions

The manuscript was written through contributions of all authors. All authors have given approval to the final version of the manuscript.

Funding

This work was supported by NSF-CAREER Grant CHE-1150727 and NSF-RUI Grant CHE-1800080 to CHL, and by NIH Grants 2R15GM120704-01 and -02 to L.K.C..

Notes

The authors declare no competing financial interest.

ACKNOWLEDGMENTS

The authors gratefully acknowledge productive and illuminating discussion with Dr. Scott Brewer (Franklin and Marshall College) and advice on organic synthesis and assistance with stop codon suppression techniques from the group of Dr. Ryan Mehl (Oregon State University).

REFERENCES

(1) Decatur, S. M. Elucidation of Residue-Level Structure and Dynamics of Polypeptides via Isotope-Edited Infrared Spectroscopy. *Acc. Chem. Res.* **2006**, *39*, 169−175.

(2) Barber-Armstrong, W.; Donaldson, T.; Wijesooriya, H.; Silva, R.; Decatur, S. M. Empirical Relationships between Isotope-Edited IR Spectra and Helix Geometry in Model Peptides. *J. Am. Chem. Soc.* **2004**, *126*, 2339−2345.

(3) Setnicka, V.; Huang, R.; Thomas, C. L.; Etienne, M. A.; Kubelka, J.; Hammer, R. P.; Keiderling, T. A. IR Study of Cross-Strand Coupling in a Beta-Hairpin Peptide Using Isotopic Labels. *J. Am. Chem. Soc.* **2005**, *127*, 4992−4993.

(4) Huang, R.; Kubelka, J.; Barber-Armstrong, W.; Silva, R.; Decatur, S.; Keiderling, T. Nature of Vibrational Coupling in Helical Peptides: An Isotopic Labeling Study. *J. Am. Chem. Soc.* **2004**, *126*, 2346−2354.

(5) Lakhani, A.; Roy, A.; De Poli, M.; Nakaema, M.; Formaggio, F.; Toniolo, C.; Keiderling, T. A. Experimental and Theoretical Spectroscopic Study of 3(10)-Helical Peptides Using Isotopic Labeling to Evaluate Vibrational Coupling. *J. Phys. Chem. B* **2011**, *115* (19), 6252−6264.

(6) Silva, R.; Kubelka, J.; Bour, P.; Decatur, S. M.; Keiderling, T. A. Site-Specific Conformational Determination in Thermal Unfolding Studies of Helical Peptides Using Vibrational Circular Dichroism with

Isotopic Substitution. *Proc. Natl. Acad. Sci. U. S. A.* **2000**, *97*, 8318−8323.
(7) Londergan, C. H.; Wang, J. P.; Axelsen, P. H.; Hochstrasser, R. M. Two-Dimensional Infrared Spectroscopy Displays Signatures of Structural Ordering in Peptide Aggregates. *Biophys. J.* **2006**, *90*, 4672−4685.
(8) Buchanan, L. E.; Dunkelberger, E. B.; Tran, H. Q.; Cheng, P.-N.; Chiu, C.-C.; Cao, P.; Raleigh, D. P.; de Pablo, J. J.; Nowick, J. S.; Zanni, M. T. Mechanism of IAPP Amyloid Fibril Formation Involves an Intermediate with a Transient β-Sheet. *Proc. Natl. Acad. Sci. U. S. A.* **2013**, *110* (48), 19285−19290.
(9) Woys, A. M.; Lin, Y.-S.; Reddy, A. S.; Xiong, W.; de Pablo, J. J.; Skinner, J. L.; Zanni, M. T. 2D IR Line Shapes Probe Ovispirin Peptide Conformation and Depth in Lipid Bilayers. *J. Am. Chem. Soc.* **2010**, *132* (8), 2832−2838.
(10) Huang, C.-Y.; Getahun, Z.; Wang, T.; DeGrado, W. F.; Gai, F. Time-Resolved Infrared Study of the Helix−Coil Transition Using 13C-Labeled Helical Peptides. *J. Am. Chem. Soc.* **2001**, *123* (48), 12111−12112.
(11) Adhikary, R.; Zimmermann, J.; Liu, J.; Dawson, P. E.; Romesberg, F. E. Experimental Characterization of Electrostatic and Conformational Heterogeneity in an SH3 Domain. *J. Phys. Chem. B* **2013**, *117* (42), 13082−13089.
(12) Chin, J. K.; Jimenez, R.; Romesberg, F. E. Direct Observation of Protein Vibrations by Selective Incorporation of Spectroscopically Observable Carbon-Deuterium Bonds in Cytochrome c. *J. Am. Chem. Soc.* **2001**, *123*, 2426−2427.
(13) Cremeens, M.; Fujisaki, H.; Zhang, Y.; Zimmermann, J.; Sagle, L.; Matsuda, S.; Dawson, P.; Straub, J.; Romesberg, F. Efforts toward Developing Direct Probes of Protein Dynamics. *J. Am. Chem. Soc.* **2006**, *128*, 6028−6029.
(14) Groff, D.; Thielges, M. C.; Cellitti, S.; Schultz, P. G.; Romesberg, F. E. Efforts Toward the Direct Experimental Characterization of Enzyme Microenvironments: Tyrosine100 in Dihydrofolate Reductase. *Angew. Chem.-Int. Ed.* **2009**, *48*, 3478−3481.
(15) Naraharisetty, S. R. G.; Kasyanenko, V. M.; Zimmermann, J.; Thielges, M. C.; Romesberg, F. E.; Rubtsov, I. V. C-D Modes of Deuterated Side Chain of Leucine as Structural Reporters via Dual-Frequency Two-Dimensional Infrared Spectroscopy. *J. Phys. Chem. B* **2009**, *113*, 4940−4946.
(16) Sagle, L. B.; Zimmermann, J.; Dawson, P. E.; Romesberg, F. E. Direct and High Resolution Characterization of Cytochrome c Equilibrium Folding. *J. Am. Chem. Soc.* **2006**, *128*, 14232−14233.
(17) Yu, W.; Dawson, P. E.; Zimmermann, J.; Romesberg, F. E. Carbon-Deuterium Bonds as Probes of Protein Thermal Unfolding. *J. Phys. Chem. B* **2012**, *116* (22), 6397−6403.
(18) Zimmermann, J.; Thielges, M. C.; Yu, W.; Dawson, P. E.; Romesberg, F. E. Carbon-Deuterium Bonds as Site-Specific and Nonperturbative Probes for Time-Resolved Studies of Protein Dynamics and Folding. *J. Phys. Chem. Lett.* **2011**, *2*, 412−416.
(19) Hoffman, K. W.; Romei, M. G.; Londergan, C. H. A New Raman Spectroscopic Probe of Both the Protonation State and Noncovalent Interactions of Histidine Residues. *J. Phys. Chem. A* **2013**, *117* (29), 5987−5996.
(20) Moran, S. D.; Woys, A. M.; Buchanan, L. E.; Bixby, E.; Decatur, S. M.; Zanni, M. T. Two-Dimensional IR Spectroscopy and Segmental C-13 Labeling Reveals the Domain Structure of Human Gamma D-Crystallin Amyloid Fibrils. *Proc. Natl. Acad. Sci. U. S. A.* **2012**, *109* (9), 3329−3334.
(21) Moran, S. D.; Decatur, S. M.; Zanni, M. T. Structural and Sequence Analysis of the Human Gamma D-Crystallin Amyloid Fibril Core Using 2D IR Spectroscopy, Segmental C-13 Labeling, and Mass Spectrometry. *J. Am. Chem. Soc.* **2012**, *134* (44), 18410−18416.
(22) Waegele, M. M.; Culik, R. M.; Gai, F. Site-Specific Spectroscopic Reporters of the Local Electric Field, Hydration, Structure, and Dynamics of Biomolecules. *J. Phys. Chem. Lett.* **2011**, *2* (20), 2598−2609.
(23) Ma, J.; Pazos, I. M.; Zhang, W.; Culik, R. M.; Gai, F. Site-Specific Infrared Probes of Proteins. *Annu. Rev. Phys. Chem.* **2015**, *66* (1), 357−377.
(24) Getahun, Z.; Huang, C. Y.; Wang, T.; De Leon, B.; DeGrado, W. F.; Gai, F. Using Nitrile-Derivatized Amino Acids as Infrared Probes of Local Environment. *J. Am. Chem. Soc.* **2003**, *125* (2), 405−411.
(25) Tucker, M. J.; Kim, Y. S.; Hochstrasser, R. M. 2D IR Photon Echo Study of the Anharmonic Coupling in the OCN Region of Phenyl Cyanate. *Chem. Phys. Lett.* **2009**, *470* (1−3), 80−84.
(26) Fafarman, A. T.; Webb, L. J.; Chuang, J. I.; Boxer, S. G. Site-Specific Conversion of Cysteine Thiols into Thiocyanate Creates an IR Probe for Electric Fields in Proteins. *J. Am. Chem. Soc.* **2006**, *128*, 13356−13357.
(27) Choi, J. H.; Raleigh, D.; Cho, M. Azido Homoalanine Is a Useful Infrared Probe for Monitoring Local Electrostatistics and Side-Chain Solvation in Proteins. *J. Phys. Chem. Lett.* **2011**, *2*, 2158−2162.
(28) Smith, E. E.; Linderman, B. Y.; Luskin, A. C.; Brewer, S. H. Probing Local Environments with the Infrared Probe: L-4-Nitrophenylalanine. *J. Phys. Chem. B* **2011**, *115* (10), 2380−2385.
(29) Woys, A. M.; Mukherjee, S. S.; Skoff, D. R.; Moran, S. D.; Zanni, M. T. A Strongly Absorbing Class of Non-Natural Labels for Probing Protein Electrostatics and Solvation with FTIR and 2D IR Spectroscopies. *J. Phys. Chem. B* **2013**, *117* (17), 5009−5018.
(30) King, J. T.; Kubarych, K. J. Site-Specific Coupling of Hydration Water and Protein Flexibility Studied in Solution with Ultrafast 2D-IR Spectroscopy. *J. Am. Chem. Soc.* **2012**, *134* (45), 18705−18712.
(31) Thielges, M. C. Transparent Window 2D IR Spectroscopy of Proteins. *J. Chem. Phys.* **2021**, *155* (4), 040903.
(32) Flynn, J. D.; Gimmen, M. Y.; Dean, D. N.; Lacy, S. M.; Lee, J. C. Terminal Alkynes as Raman Probes of α-Synuclein in Solution and in Cells. *ChemBioChem* **2020**, *21*, 1582−1586.
(33) Wei, L.; Hu, F.; Shen, Y.; Chen, Z.; Yu, Y.; Lin, C.-C.; Wang, M. C.; Min, W. Live-Cell Imaging of Alkyne-Tagged Small Biomolecules by Stimulated Raman Scattering. *Nat. Methods* **2014**, *11* (4), 410−412.
(34) Azemtsop Matanfack, G.; Rüger, J.; Stiebing, C.; Schmitt, M.; Popp, J. Imaging the Invisible—Bioorthogonal Raman Probes for Imaging of Cells and Tissues. *J. Biophotonics* **2020**, *13* (9), e202000129.
(35) Weeks, C. L.; Polishchuk, A.; Getahun, Z.; DeGrado, W. F.; Spiro, T. G. Investigation of an Unnatural Amino Acid for Use as a Resonance Raman Probe: Detection Limits and Solvent and Temperature Dependence of the NC≡N Band of 4-Cyanophenylalanine. *J. Raman Spectrosc.* **2008**, *39* (11), 1606−1613.
(36) Yamakoshi, H.; Dodo, K.; Palonpon, A.; Ando, J.; Fujita, K.; Kawata, S.; Sodeoka, M. Alkyne-Tag Raman Imaging for Visualization of Mobile Small Molecules in Live Cells. *J. Am. Chem. Soc.* **2012**, *134*, 20681−20689.
(37) Chen, Z.; Paley, D. W.; Wei, L.; Weisman, A. L.; Friesner, R. A.; Nuckolls, C.; Min, W. Multicolor Live-Cell Chemical Imaging by Isotopically Edited Alkyne Vibrational Palette. *J. Am. Chem. Soc.* **2014**, *136* (22), 8027−8033.
(38) Alaune, Z.; Mozolis, V. Spectra of Acetylenic Compounds. *Liet. TSR Mokslu Akad Darb. Ser. B* **1963**, 101−105.
(39) Alaune, Z.; Talaikyte, Z. Investigation of the Intensity in the Vibrational Spectra of Conjugated Acetylenic Compounds. *Liet. TSR Mokslu Akad Darb. Ser. B* **1964**, 57−64.
(40) Alaune, Z.; Talaikyte, Z. Spectral Studies of Acetylenic Compounds. *Liet. TSR Mokslu Akad. Darb. Ser. B Chem. Technol. Fiz. Geogr.* **1967**, 55−66.
(41) Palonpon, A. F.; Ando, J.; Yamakoshi, H.; Dodo, K.; Sodeoka, M.; Kawata, S.; Fujita, K. Raman and SERS Microscopy for Molecular Imaging of Live Cells. *Nat. Protoc.* **2013**, *8*, 677−692.
(42) Yamakoshi, H.; Dodo, K.; Okada, M.; Ando, J.; Palonpon, A.; Fujita, K.; Kawata, S.; Sodeoka, M. Imaging of EdU, an Alkyne-Tagged Cell Proliferation Probe, by Raman Microscopy. *J. Am. Chem. Soc.* **2011**, *133*, 6102−6105.

https://doi.org/10.1021/acs.jpcb.2c06176
J. Phys. Chem. B 2023, 127, 85−94

(43) Palonpon, A. F.; Sodeoka, M.; Fujita, K. Molecular Imaging of Live Cells by Raman Microscopy. *Curr. Opin. Chem. Biol.* **2013**, *17*, 708−715.
(44) Bakthavatsalam, S.; Dodo, K.; Sodeoka, M. A Decade of Alkyne-Tag Raman Imaging (ATRI): Applications in Biological Systems. *RSC Chem. Biol.* **2021**, *2* (5), 1415−1429.
(45) Ando, J.; Palonpon, A. F.; Sodeoka, M.; Fujita, K. High-Speed Raman Imaging of Cellular Processes. *Curr. Opin. Chem. Biol.* **2016**, *33*, 16−24.
(46) Chen, C.; Zhao, Z.; Qian, N.; Wei, S.; Hu, F.; Min, W. Multiplexed Live-Cell Profiling with Raman Probes. *Nat. Commun.* **2021**, *12* (1), 3405.
(47) Hu, F.; Shi, L.; Min, W. Biological Imaging of Chemical Bonds by Stimulated Raman Scattering Microscopy. *Nat. Methods* **2019**, *16* (9), 830−842.
(48) Du, J.; Wei, L. Multicolor Photoactivatable Raman Probes for Subcellular Imaging and Tracking by Cyclopropenone Caging. *J. Am. Chem. Soc.* **2022**, *144* (2), 777−786.
(49) Bi, X.; Miao, K.; Wei, L. Alkyne-Tagged Raman Probes for Local Environmental Sensing by Hydrogen−Deuterium Exchange. *J. Am. Chem. Soc.* **2022**, *144* (19), 8504−8514.
(50) Egoshi, S.; Dodo, K.; Ohgane, K.; Sodeoka, M. Deuteration of Terminal Alkynes Realizes Simultaneous Live Cell Raman Imaging of Similar Alkyne-Tagged Biomolecules. *Org. Biomol. Chem.* **2021**, *19* (38), 8232−8236.
(51) Miao, Y.; Shi, L.; Hu, F.; Min, W. Probe Design for Super-Multiplexed Vibrational Imaging. *Phys. Biol.* **2019**, *16* (4), 041003.
(52) Epstein, S. C.; Huff, A. R.; Winesett, E. S.; Londergan, C. H.; Charkoudian, L. K. Tracking Carrier Protein Motions with Raman Spectroscopy. *Nat. Commun.* **2019**, *10* (1), 1−6.
(53) Kossowska, D.; Lee, G.; Han, H.; Kwak, K.; Cho, M. Simultaneous Enhancement of Transition Dipole Strength and Vibrational Lifetime of an Alkyne IR Probe via π-d Backbonding and Vibrational Decoupling. *Phys. Chem. Chem. Phys.* **2019**, *21* (45), 24919−24925.
(54) Kossowska, D.; Park, K.; Park, J. Y.; Lim, C.; Kwak, K.; Cho, M. Rational Design of an Acetylenic Infrared Probe with Enhanced Dipole Strength and Increased Vibrational Lifetime. *The Journal of Physical Chemistry B* **2019**, *123*, 6274−6281.
(55) Kolb, H. C.; Finn, M. G.; Sharpless, K. B. Click Chemistry: Diverse Chemical Function from a Few Good Reactions. *Angew. Chem.-Int. Ed.* **2001**, *40* (11), 2004−2021.
(56) van Hest, J. C. M.; Kiick, K. L.; Tirrell, D. A. Efficient Incorporation of Unsaturated Methionine Analogues into Proteins in Vivo. *J. Am. Chem. Soc.* **2000**, *122* (7), 1282−1288.
(57) Schultz, K. C.; Supekova, L.; Ryu, Y. H.; Xie, J. M.; Perera, R.; Schultz, P. G. A Genetically Encoded Infrared Probe. *J. Am. Chem. Soc.* **2006**, *128*, 13984−13985.
(58) Miyake-Stoner, S. J.; Miller, A. M.; Hammill, J. T.; Peeler, J. C.; Hess, K. R.; Mehl, R. A.; Brewer, S. H. Probing Protein Folding Using Site-Specifically Encoded Unnatural Amino Acids as FRET Donors with Tryptophan. *Biochemistry* **2009**, *48* (25), 5953−5962.
(59) Blasiak, B.; Lee, H.; Cho, M. Vibrational Solvatochromism: Towards Systematic Approach to Modeling Solvation Phenomena. *J. Chem. Phys.* **2013**, *139* (4), 044111.
(60) Blasiak, B.; Cho, M. Vibrational Solvatochromism. II. A First-Principle Theory of Solvation-Induced Vibrational Frequency Shift Based on Effective Fragment Potential Method. *J. Chem. Phys.* **2014**, *140* (16), 164107.
(61) Blasiak, B.; Cho, M. Vibrational Solvatochromism. III. Rigorous Treatment of the Dispersion Interaction Contribution. *J. Chem. Phys.* **2015**, *143* (16), 164111.
(62) Fafarman, A. T.; Sigala, P. A.; Herschlag, D.; Boxer, S. G. Decomposition of Vibrational Shifts of Nitriles into Electrostatic and Hydrogen-Bonding Effects. *J. Am. Chem. Soc.* **2010**, *132*, 12811−12813.
(63) Bagchi, S.; Fried, S. D.; Boxer, S. G. A Solvatochromic Model Calibrates Nitriles' Vibrational Frequencies to Electrostatic Fields. *J. Am. Chem. Soc.* **2012**, *134* (25), 10373−10376.
(64) Fried, S. D.; Boxer, S. G. Measuring Electric Fields and Noncovalent Interactions Using the Vibrational Stark Effect. *Acc. Chem. Res.* **2015**, *48* (4), 998−1006.
(65) Wolfshorndl, M. P.; Baskin, R.; Dhawan, I.; Londergan, C. H. Covalently Bound Azido Groups Are Very Specific Water Sensors, Even in Hydrogen-Bonding Environments. *J. Phys. Chem. B* **2012**, *116* (3), 1172−1179.
(66) Pogostin, B. H.; Malmendal, A.; Londergan, C. H.; Åkerfeldt, K. S. PKa Determination of a Histidine Residue in a Short Peptide Using Raman Spectroscopy. *Molecules* **2019**, *24* (3), 405.
(67) Koppel, I. A.; Palm, V. A. Chapter 5. In *Advances in Linear Free Energy Relationships*; Plenum Press: New York, 1972.
(68) Onsager, L. Electric Moments of Molecules in Liquids. *J. Am. Chem. Soc.* **1936**, *58*, 1486−1493.
(69) Błasiak, B.; Londergan, C. H.; Webb, L. J.; Cho, M. Vibrational Probes: From Small Molecule Solvatochromism Theory and Experiments to Applications in Complex Systems. *Acc. Chem. Res.* **2017**, *50* (4), 968−976.
(70) Laurence, C.; Legros, J.; Chantzis, A.; Planchat, A.; Jacquemin, D. A Database of Dispersion-Induction DI, Electrostatic ES, and Hydrogen Bonding A1 and B1 Solvent Parameters and Some Applications to the Multiparameter Correlation Analysis of Solvent Effects. *J. Phys. Chem. B* **2015**, *119* (7), 3174−3184.
(71) Lindquist, B. A.; Furse, K. E.; Corcelli, S. A. Nitrile Groups as Vibrational Probes of Biomolecular Structure and Dynamics: An Overview. *Phys. Chem. Chem. Phys.* **2009**, *11*, 8119−8132.
(72) Roujeinikova, A.; Simon, W. J.; Gilroy, J.; Rice, D. W.; Rafferty, J. B.; Slabas, A. R. Structural Studies of Fatty Acyl-(Acyl Carrier Protein) Thioesters Reveal a Hydrophobic Binding Cavity That Can Expand to Fit Longer Substrates. *J. Mol. Biol.* **2007**, *365* (1), 135−145.
(73) Taskent-Sezgin, H.; Chung, J.; Patsalo, V.; Miyake-Stoner, S. J.; Miller, A. M.; Brewer, S. H.; Mehl, R. A.; Green, D. F.; Raleigh, D. P.; Carrico, I. Interpretation of P-Cyanophenylalanine Fluorescence in Proteins in Terms of Solvent Exposure and Contribution of Side-Chain Quenchers: A Combined Fluorescence, IR and Molecular Dynamics Study. *Biochemistry* **2009**, *48*, 9040−9046.
(74) Kean, K. M.; van Zee, K.; Mehl, R. A. Unnatural Chemical Biology: Research-Based Laboratory Course Utilizing Genetic Code Expansion. *J. Chem. Educ.* **2019**, *96* (1), 66−74.

https://doi.org/10.1021/acs.jpcb.2c06176
J. Phys. Chem. B 2023, 127, 85−94